0026-895X/06/6904-1468–1476$20.00
MOLECULAR PHARMACOLOGY
Vol. 69, No. 4
20594/3100881

Mol Pharmacol 69:1468–1476, 2006
Printed in U.S.A.

The Contribution of TWIK-Related Acid-Sensitive K^+-Containing Channels to the Function of Dorsal Lateral Geniculate Thalamocortical Relay Neurons

Sven G. Meuth, M. Isabel Aller, Thomas Munsch, Thekla Schuhmacher, Thomas Seidenbecher, Patrick Meuth, Christoph Kleinschnitz, Hans-Christian Pape, Heinz Wiendl, William Wisden, and Thomas Budde

Institut für Experimentelle Epilepsieforschung, Westfälische Wilhelms-Universität Münster, Münster, Germany (T.B., H.-C.P.); Abteilung für Klinische Neurobiologie, Universität Heidelberg, Heidelberg, Germany (M.I.A., W.W.); Institut für Physiologie, Otto-von-Guericke-Universität, Magdeburg, Germany (T.M.); Institut für Physiologie I, Westfälische Wilhelms-Universität Münster, Münster, Germany (T.Se., H.-C.P.); Klinik für Neurologie, Julius-Maximilians-Universität Würzburg, Würzburg, Germany (S.G.M., T.Sc., C.K., H.W.); and Institute of Medical Sciences, University of Aberdeen, Foresterhill, Aberdeen, Scotland, United Kingdom (W.W.)

Received November 8, 2005; accepted January 18, 2006

ABSTRACT

A genetic knockout was used to determine the specific contribution of TWIK-related acid-sensitive K^+ (TASK)-1 channels to the function of dorsal lateral geniculate nucleus (DLG) thalamocortical relay (TC) neurons. Disruption of TASK-1 function produced an ~19% decrease in amplitude of the standing outward current (I_{SO}) and a 3 ± 1-mV depolarizing shift in resting membrane potential (V_{rest}) of DLG neurons. We estimated that current through TASK-1 homodimers or TASK-1/TASK-3 heterodimers contribute(s) approximately one third of the current sensitive to TASK channel modulators in DLG TC neurons. The effects of the TASK channel blocker bupivacaine (20 μM), of muscarine (50 μM), and of H^+ on I_{SO} were reduced to approximately 60%, 59%, and shifted to more acidic pH values, respectively. The blocking effect of anandamide on I_{SO} [30 μM; 23 ± 3% current decrease in wild type (WT)] was absent in TASK-1 knockout (TASK-$1^{-/-}$) mice (9 ± 6% current increase). Comparable results were obtained with the more stable anandamide derivative methanandamide (20 μM; 20 ± 2% decrease in WT; 4 ± 6% increase in TASK-$1^{-/-}$). Current-clamp recordings revealed a muscarine-induced shift in TC neuron activity from burst to tonic firing in both mouse genotypes. Electrocorticograms and sleep/wake times were unchanged in TASK-$1^{-/-}$ mice. In conclusion, our findings demonstrate a significant contribution of TASK-1 channels to I_{SO} in DLG TC neurons, although the genetic knockout of TASK-1 did not produce severe deficits in the thalamocortical system.

K2P potassium channels contribute to the leak conductance that helps maintain negative resting membrane potentials (Brown, 2000; Lesage and Lazdunski, 2000; Patel and Honore, 2001). The 15 mammalian K2P channel proteins are divided into six subfamilies based on sequence identities and functional features (Patel and Lazdunski, 2004). K2P subunits assemble as dimers (Plant et al., 2005), and some may be heterodimers. Whereas some channel subunits mediate time- and voltage-independent potassium leak currents, other subtypes, including TASK channels, increase their open probability with depolarization. Most K2P channels can be actively modulated; for example, many neurotransmitters/neuromodulators act via G protein-coupled receptors to close TASK channels and so depolarize the cell, producing a change from burst to tonic firing in DLG neurons (Millar et al., 2000; Talley et al., 2000; Meuth et al., 2003).

The current through TASK-1 and -3 subunits reveals outward rectification of whole-cell currents under physiological

This work was supported by Deutsche Forschungsgemeinschaft grants BU 1019/5-2 (to T.B.) and WI 1951/1-2 (to W.W.), Leibniz-program (to H.-C.P.), the Volkswagen Stiftung I/78 554 (to W.W.), and Fonds der Chemischen Industrie (to W.W.).

Article, publication date, and citation information can be found at http://molpharm.aspetjournals.org.

doi:10.1124/mol.105.020594.

ABBREVIATIONS: K2P, two-pore domain potassium channel; TASK, TWIK-related acid sensitive K^+ channel; DLG, dorsal lateral geniculate nucleus; PIPES, piperazine-*N*,*N*′-bis(2-ethanesulfonic acid); BAPTA, 1,2-bis(2-aminophenoxy)ethane-*N*,*N*,*N*′,*N*′-tetraacetic acid; ECoG, electrocorticogram; TC, thalamocortical relay neuron; ACh, acetylcholine; pH_O, external pH; E_K, K^+ equilibrium potential; mAChR, muscarinic acetylcholine receptor; EEG, electroencephalogram; *R*-(+)-WIN 55,212-2, (*R*)-(+)-[2,3-dihydro-5-methyl-3-(4-morpholinylmethyl) pyrrolo-[1,2,3-*d*,*e*]-1,4-benzoxazin-6-yl]-1-naphthalenyl-methanone; ZD7288, 4-(*N*-ethyl-*N*-phenylamino)-1,2-dimethyl-6-(methylamino) pyridinium chloride.

K^+ concentrations and is inhibited by acidic pH; in recombinant systems and in vivo, channel subunits can assemble heteromerically if the cell type expresses both genes at suitable levels (Czirjak and Enyedi, 2002; Berg et al., 2004; Kang et al., 2004; Aller et al., 2005); alternatively, they can function as homomers if either TASK-1 or TASK-3 dominates the expression (Czirjak and Enyedi, 2003; Clarke et al., 2004). Because of 1) overlapping gene expression patterns, 2) similarities of whole-cell currents through different channel subtypes, and 3) the formation of heterodimeric channels resulting in intermediate properties, it is hard to specify the molecular origins of native leak currents. Thus, knockout mice are valuable to assess the in vivo contributions and functional roles of specific K2P channel subtypes.

For example, previous work with TASK-1 knockout mice (TASK-$1^{-/-}$) dissected K2P channel diversity in adult cerebellar granule cells (Aller et al., 2005). Granule cells strongly express four K2P genes: TASK-1, TASK-3, the TWIK-related K^+ channel gene-2c splice variant, and tandem pore domain halothane-inhibited K^+ channel-2. In TASK-1 knockout mice, although the standing outward K^+ current (I_{KSO}) remained unchanged, and granule cells were not more depolarized, the I_{KSO} became Zn^{2+}-sensitive, suggesting that normally most TASK channels in granule cells are TASK-1/TASK-3 heteromers, and that in the TASK-$1^{-/-}$ granule cells, this heteromer was replaced by homomeric TASK-3 channels. The failure to see a reduction in I_{KSO} magnitude in the TASK-$1^{-/-}$ granule cells could be because of contributions from the remaining K2P genes.

By contrast, not all neuronal cell types express the high K2P channel diversity found in cerebellar granule cells. For example, the main K2P genes expressed in mouse thalamus are TASK-1, TASK-3, and TWIK-1. The TASK-3 gene dominates; however, there are variations in expression depending on the exact thalamic nucleus (Fig. 1). The DLG in the mouse thalamus contains moderate levels of TASK-3 and TASK-1 transcripts, together with some TWIK-1 and other K2P gene transcripts (Aller et al., 2005); indeed, in postnatal day 19 rat DLG cells in slices, both TASK-1 and TASK-3 channels (as assayed by pharmacology and in situ hybridization) significantly contribute to the unique features of the cells (Meuth et al., 2003), although under certain circumstances (removal of covalently attached Small Ubiquitin-like Modifier protein), TWIK-1 has TASK-like channel properties (Rajan et al., 2005). Furthermore, in addition to the contribution from TASK channels, I_{SO} in TC neurons is carried by additional channel types (persistent Na^+ channels, inward rectifying K^+ channels, noninactivating voltage-dependent K^+ channels, and pacemaker channels; S. G. Meuth and T. Budde, unpublished observations). Regardless, removing expression of a particular K2P family member from any given thalamic relay nucleus might have stronger impact on function than in cerebellar granule cells, simply because there are fewer other K2P channel types expressed in the thalamus that could compensate for the loss.

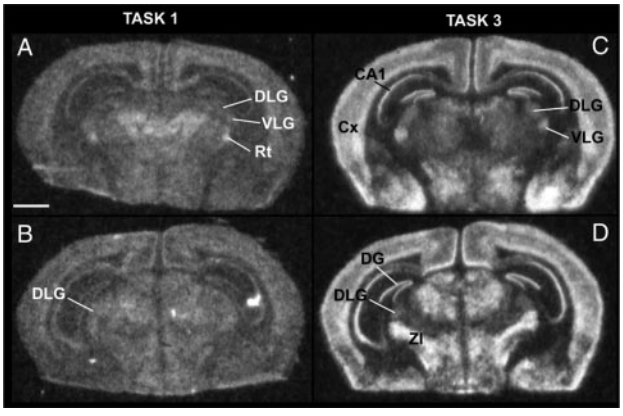

Fig. 1. In situ hybridization showing TASK-1 (A and B) and TASK-3 (C and D) gene expression in the mouse (wild-type) thalamus from P19, an age matching the electrophysiological recordings. CA1, hippocampal CA1 region; Cx, neocortex; DG, dentate granule cells; Rt, reticular thalamus; VLG, ventral lateral geniculate nucleus; and ZI, zona incerta. X-ray film autoradiographs, exposure time 4 weeks. Scale bar, 1 mm.

The likely function for K2P channels in thalamic relay cells is characterized by the closure of TASK-1 and -3 channels mediated by modulatory transmitters such as acetylcholine acting via G proteins, thereby promoting membrane depolarization and a shift in activity mode from burst to tonic firing of action potentials (McCormick, 1992; Steriade et al., 1997; Meuth et al., 2003). To determine the specific contribution of the two TASK subunit variants to the physiology of DLG TC neurons and to analyze their influences on cell's response to cholinergic modulation, we used TASK-1-deficient mice (TASK-$1^{-/-}$) (Aller et al., 2005). We addressed the following questions: 1) What are the pharmacological and functional consequences of a TASK-1 knockout in DLG cells and does it differ in its effects from cerebellar granule cells? and 2) Is there a TASK-$1^{-/-}$ phenotype related to the thalamocortical system?

Methods and Materials

The TASK-1 Knockout Mouse Line. The generation of TASK-$1^{-/-}$ mice has recently been described (Aller et al., 2005). For the study described here, and as in Aller et al. (2005), TASK-$1^{-/-}$ mice were always produced by breeding heterozygote +/− animals; the −/− and +/+ littermates could then be used for direct comparisons. Mice were genotyped by Southern blotting (Aller et al., 2005).

Animals. Mice were individually housed in standard cages without running wheels on a 12-h light/dark cycle at an ambient temperature of 23 ± 1°C. Rodent laboratory chow and drinking water were provided ad libitum. All procedures involving the use of animals were approved by the local Animal Care Committee of the Universities of Heidelberg and Magdeburg in agreement with the German laws for animal protection.

In Situ Hybridization. In situ hybridization, with ^{35}S-labeled TASK-1- and TASK-3-specific oligonucleotide probes was performed as described previously (Aller et al., 2005). Brains were from wild-type P19 animals.

Preparation: Thalamic Slices. Wild-type (WT) and TASK-$1^{-/-}$ mice postnatal day 14 to 22 were deeply anesthetized using halothane and decapitated as described previously for rats (Meuth et al., 2003). In brief, thalamic slices were prepared as coronal sections on a vibratome (Series 1000 Classic; Vibratome Company, St. Louis, MO) in an ice-chilled solution containing 200 mM sucrose, 20 mM PIPES, 2.5 mM KCl, 1.25 mM NaH_2PO_4, 10 mM $MgSO_4$, 0.5 mM $CaCl_2$, and 10 mM dextrose, pH 7.35 adjusted with NaOH. Before the recording procedure, slices were kept submerged in artificial cerebrospinal fluid: 125 mM NaCl, 2.5 mM KCl, 1.25 mM NaH_2PO_4, 24 mM $NaHCO_3$, 2 mM $MgSO_4$, 2 mM $CaCl_2$, and 10 mM dextrose, pH adjusted to 7.35 by bubbling with a mixture of 95% O_2 and 5% CO_2.

Patch-Clamp Recordings of DLG Neurons. DLG neurons were visualized in the slice preparation using a microscope equipped with infrared differential interference contrast optics. Whole-cell recording pipettes were prepared from borosilicate glass (GT150T-

10; Clark Electromedical Instruments, Pangbourne, UK) having typical resistances of 2 to 3 MΩ. Pipettes were filled with an intracellular solution containing 95 mM K-gluconate, 20 mM K_3-citrate, 10 mM NaCl, 10 mM HEPES, 1 mM $MgCl_2$, 0.5 mM $CaCl_2$, 3 mM BAPTA, 2 mM Mg-ATP, and 0.5 mM Na-GTP. In divalent cation-free external solutions the osmolarity was kept constant at 305 mOsm/kg by adding mannitol. The internal solution was set to pH 7.25 with KOH and an osmolarity of 295 mOsmol/kg. For current-clamp recordings, a pipette solution containing 5 mM EGTA and 0.5 mM $CaCl_2$ was used. Slices were continuously superfused with a solution containing 120 mM NaCl, 2.5 mM KCl, 1.25 mM NaH_2PO_4, 30 mM HEPES, 2 mM $MgSO_4$, 2 mM $CaCl_2$, and 10 mM dextrose and pH values were adjusted using HCl. Whole-cell patch-clamp recordings were measured with an EPC-10 amplifier (HEKA Elektronik, Lamprecht, Germany), digitized, and acquired onto computer using Pulse software (HEKA Elektronik).

All cells had a resting membrane potential more negative than −65 mV, the access resistance was in the range of 5 to 15 MΩ, and series resistance compensation of more than 40% was routinely used. A liquid junction potential of 8 ± 2 mV (n = 10) was measured and taken into account.

The pH response curve of the standing outward current at −28 mV was drawn according to the equation $I_{SO} = I_{max}/\{1 + (EC_{50}/A)^{nH}\}$, where I_{SO} represents the current response, I_{max} is the maximal relative current amplitude, EC_{50} is the half-maximal effective pH value, A is the pH value, and n_H is the Hill coefficient.

Drugs. The following drugs were used for electrophysiological recordings: bupivacaine and muscarine were obtained from Sigma Chemie (Deisenhofen, Germany), prepared as stock solutions in distilled water, and added to the perfusion medium. ZD7288 was delivered from Tocris Cookson Inc. (Köln, Germany) and prepared as described above. Anandamide, methanandamide, and arachidonic acid were obtained from Calbiochem (Schwalbach/Ts., Germany) and dissolved in ethanol. The solvent concentration in the final recording solution did not exceed 1%. Application of the solvent alone (1%) had no effect on the recorded current.

Surgery and Electrode Implantation. Experiments were performed on male mice (between 8 and 12 weeks old; n = 5 for TASK-$1^{-/-}$- and wild-type littermates, respectively) and were approved by the Landesverwaltungsamt Halle (AZ 2–663Uni Magdeburg). After anesthesia with pentobarbital (50 mg/kg i.p.; Sigma Chemical Co., St. Louis, MO), the mouse was positioned in a stereotaxic instrument (David Kopf Instruments, Tujunga, CA) with bregma and lambda in a horizontal plane. For bilateral epidural electrocorticogram (ECoG) recordings, silver electrodes were positioned over the central region (AP, −1.0 mm; L, 2 mm from bregma) of both hemispheres and fixed on the skull with dental acrylic cement (Paladur; Heraeus Kulzer GmbH, Wehrheim/Ts, Germany). In addition, reference and ground electrodes were implanted over the nasal and cerebellar region, respectively. Xylocaine cream (2%; Astra GmbH, Germany) was applied to all pressure points and wound edges. Four days after surgery, ECoG was recorded for 4 to 6 h to get a wide spectrum of different behavioral states (i.e., wake and sleep) using a swivel commutator.

ECoG recordings were performed using the spike2-software package (Cambridge Electronic Design, Cambridge, UK). Recorded electrical activities were fed through a differential amplifier (EXT-20F or DPA 2F; npi electronic GmbH, Tamm, Germany) collected at a sampling rate of 1 kHz with a filter cut-off of 100 Hz, transformed by an A/D interface (CED 1401plus; Cambridge Electronic Design) and stored on-line on a personal computer. In addition, data were stored on a magnetic tape recorder via a neuro-corder (DR-890; NeuroData Instr. Corp., Delaware Water Gap, PA) for off-line analysis.

Behavioral Observations. The activity of WT (n = 5; 27.58 ± 3 g) and TASK-$1^{-/-}$ mice (n = 8; 28.39 ± 1.4 g) was continuously recorded in their home cages by infrared detectors for 24 h. These recordings were analyzed by two experienced observers blinded for the genetic background of the animals. Forms of behavior (sleep, resting, leaning, rearing, grooming, nutrition, and moving) were calculated as percentage of 24 h.

Statistics. All results are presented as mean ± S.E. and differences were considered statistically significant if $p < 0.05$. Substance effects were tested for statistical significance using a modified Student's t test for small samples (Dixon and Massey, 1969).

Results

Expression of the TASK-1 and TASK-3 Genes in the Mouse DLG. We first examined the DLG by in situ hybridization and focused on the expression of the TASK-1 and -3 genes in our target thalamic nucleus. Mouse brains were selected from an age that matched the majority of electrophysiological recordings, postnatal day 19. Figure 1 shows coronal brain sections through the thalamus at the DLG level. We reported previously for the adult mouse brain (Aller et al., 2005), that the TASK-1 gene's highest expression is in cerebellar granule cells, motor neurons, raphe, and locus ceruleus, whereas TASK-3 gene expression is at higher levels throughout the brain (e.g., CA1 pyramidal cells, dentate granule cells, neocortex, and many hypothalamic nuclei). This is reflected in the coronal images shown in Fig. 1 at the level of the thalamus for P19. Nevertheless, specific thalamic nuclei have quite different expression profiles of the TASK-1 and TASK-3 genes. For example, the ventral lateral geniculate nucleus (VLG) has more TASK-3 than TASK-1 gene expression, whereas the midline thalamic nuclei have more TASK-1 transcripts (Fig. 1, A and C). More caudally (Fig. 1, B and D), TASK-3 expression dominates in the thalamus and zona incerta (Fig. 1D). TASK-1 expression dominates in the reticular thalamus (Fig. 1A). Despite the overall predominance of TASK-3 gene expression in the fore- and midbrain, both TASK-1 and TASK-3 mRNAs can be detected in the DLG at approximately roughly equal amounts (Fig. 1, A and C).

pH Sensitivity of Leak Potassium Channels in WT and TASK-$1^{-/-}$ DLG Neurons: Consequences for the Resting Membrane Potential. TASK-1 and -3 channels contribute to the I_{SO} (Fig. 3A) in several cell types, such as cerebellar granule cells, motor neurons, and DLG TC cells (Millar et al., 2000; Brickley et al., 2001; Bayliss et al., 2003; Meuth et al., 2003). To assess the contribution of the TASK-1 subunit to the total TASK-1 and -3 current in TC neurons of the DLG, we probed a number of TASK-1 and -3 channel features (pH sensitivity, block by bupivacaine, and modulation by ACh) in whole-cell patch-clamp experiments. Both TASK-1 and TASK-3 channels are inhibited by acidification, although over different pH ranges (pK values for channel activity, ~7.5 and ~6.7 for TASK-1 and TASK-3, respectively) (Duprat et al., 1997; Kim et al., 2000; Rajan et al., 2000). Tandem-linked heterodimeric TASK channel constructs displayed pH sensitivity (pK ~7.3) closer to that of TASK-1 than TASK-3 (Berg et al., 2004). In a first experimental step, we compared the pH dependence of I_{SO} in WT and TASK-$1^{-/-}$ mice. At a holding potential of −28 mV I_{SO} averaged 368 ± 17 pA in WT mice (n = 38) and 299 ± 16 pA in TASK-$1^{-/-}$ mice (n = 37; data not shown; p = 0.005) under experimental control conditions (pH 7.25). Varying the external pH (pH_O) from 8.0 to 5.0 stepwise resulted in a reduction of I_{SO}, which was different in both genotypes. Whereas I_{SO} averaged 438 ± 47 pA (n = 4) and 415 ± 32 pA (n = 3) at pH

7.5 in WT and TASK-1$^{-/-}$, respectively, current amplitudes were strongly reduced to 39 ± 22 pA (n = 4; WT) and 35 ± 29 pA (n = 3; TASK-1$^{-/-}$) at pH 5.0. From populations of cells (a total of 24 cells were tested for each genotype) recorded at different pH values, the EC_{50} value of I_{SO} inhibition could be determined at 6.6 and 5.9 for WT and TASK-1$^{-/-}$, respectively, according to the Hill equation (Fig. 2A).

Next, we determined the resting membrane potential (V_{rest}) of DLG TC neurons. In accordance with the averaged I_{SO} amplitudes and the knockout of a hyperpolarizing membrane current, V_{rest} under control conditions (pH_O = 7.25) was significantly ($p < 0.009$) more negative than in WT (−73 ± 1 mV; n = 19) compared with TASK-1$^{-/-}$ (−70 ± 1 mV; n = 10; Fig. 2B). This difference was sustained when the depolarizing pH-sensitive current through HCN channels, the I_h current, was blocked by ZD7288 (BoSmith et al., 1993) (WT, −83 ± 1 mV; n = 11; TASK$^{-/-}$, −76 ± 2 mV; n = 8; Fig. 2B). Subsequent reduction of pH_O to 5.0 resulted in strong depolarization of V_{rest} to values that were not different between the knockout and wild-type littermates (WT, −34 ± 4 mV; n = 3; TASK-1$^{-/-}$, −35 ± 3 mV; n = 4; Fig. 2B). In summary, these data indicate reduced I_{SO} amplitude and depolarized V_{rest} in DLG cells lacking TASK-1 expression.

Actions of the Local Anesthetic Bupivacaine on I_{SO} in DLG Neurons. Next, the local anesthetic bupivacaine, known to block TASK-1 and -3 channels (Leonoudakis et al., 1998; Kindler et al., 1999; Meadows and Randall, 2001; Meuth et al., 2003) was tested. Bath application of 20 μM bupivacaine resulted in a marked reduction in I_{SO} amplitude, which was significantly (p = 0.027) stronger in WT (55 ± 8%; n = 8) compared with TASK-1$^{-/-}$ (33 ± 4%; n = 8; Fig. 3, A, B, and D). To determine the current-voltage (I/V) relationship of the bupivacaine-sensitive current, the membrane potential was ramped from −28 to −138 mV over 800 ms (Fig. 3, A and B, inset). The resulting current revealed a complex waveform indicative for outwardly and inwardly rectifying components (Fig. 3, A and B). By subtracting currents in the presence of bupivacaine from control currents, and assigning the appropriate membrane potential to each time point, the I-V relationship of the bupivacaine-sensitive current was constructed (Fig. 3C). The bupivacaine-sensitive currents in DLG neurons revealed clear outward rectification and a reversal potential of −103 ± 5 (n = 8) and of −103 ± 3 (n = 8) for WT and TASK-1$^{-/-}$, respectively [i.e., close to the expected K^+ equilibrium potential (E_K) of −104 mV]. In summary, these data indicate a reduced bupivacaine-sensitive current component in DLG neurons lacking TASK-1 gene expression.

Muscarine Inhibits I_{SO} in WT and TASK-1$^{-/-}$ DLG Cells: Functional Implications. Next, we investigated the functional modulation of TASK-1 and -3 channels in DLG neurons by activation of muscarinic ACh receptors

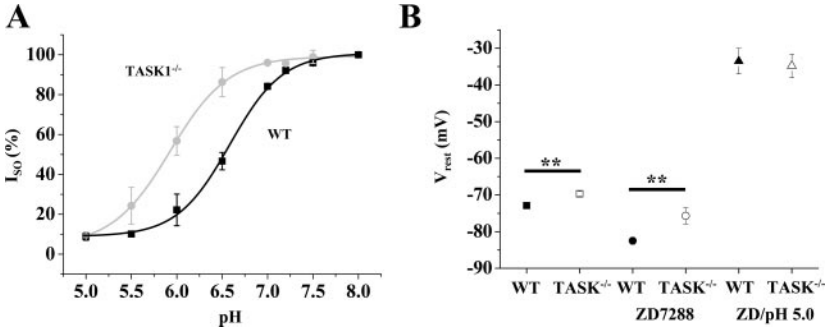

Fig. 2. pH sensitivity of the standing outward current in WT and TASK-1$^{-/-}$ DLG neurons. A, dependence of I_{SO} at −28 mV on extracellular acidification (mean ± S.E.) for groups of three to five relay neurons in a range from pH 5.0 to 8.0 is shown. The curve was drawn according to the Hill equation through the data points for WT (black line) and TASK-1$^{-/-}$ (gray line), respectively. The EC_{50}, I_{max}, and Hill values were WT, 6.6, 106.4, and 0.53; and TASK-1$^{-/-}$, 5.9, 101.4, and 0.55. B, mean value of the resting membrane potential under different recording conditions (squares, control conditions; circles, presence of ZD7288; triangles, presence of ZD7288 at pH 5.0; WT, closed symbols; TASK-1$^{-/-}$, open symbols).

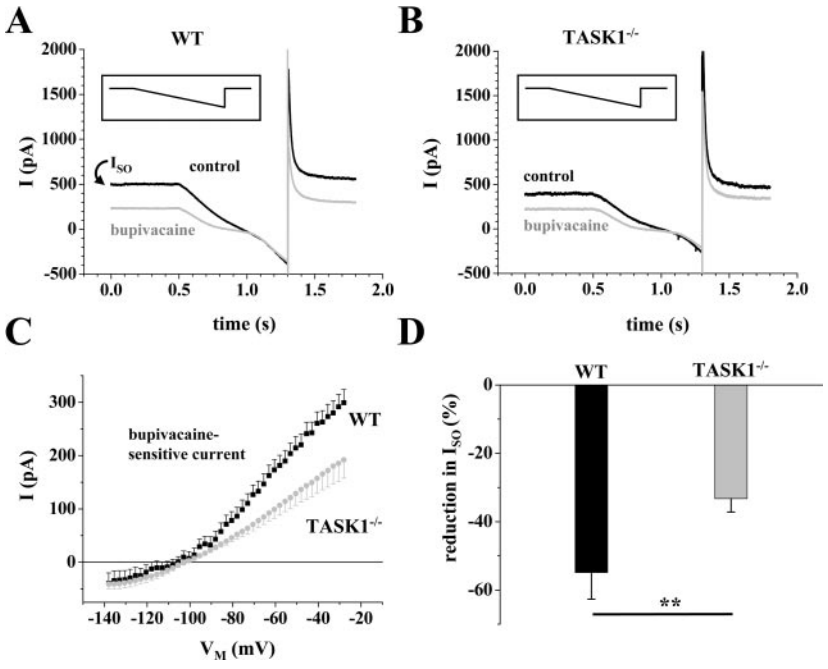

Fig. 3. Effect of bupivacaine on TASK current in WT and TASK-1$^{-/-}$ DLG neurons. A and B, currents evoked by ramping the membrane potential from −28 to −138 mV over 800 ms (see inset) under control conditions (black trace) and during application of bupivacaine (gray trace) in WT (A) and TASK-1$^{-/-}$ mice (B). C, mean I-V relationship of current components sensitive to bupivacaine obtained by graphical subtraction of currents during drug action from control currents (i.e., control − bupivacaine). Both components show a clear outward rectification and a reversal at the expected E_K. D, mean bar graph representation of I_{SO} reduction at −28 mV by bupivacaine in WT (black column) and TASK-1$^{-/-}$ (gray column).

(mAChRs). First, the action of muscarine (50 μM) was analyzed under voltage-clamp conditions. After application of muscarine via the extracellular solution, I_{SO} amplitude was significantly ($p = 0.025$) reduced by 41 ± 2% ($n = 4$) and 24 ± 4% ($n = 8$) in WT and TASK-1$^{-/-}$, respectively (Fig. 4, A, B, and D). The curvature of the muscarine-sensitive I-V relationship was characterized by inward and outward rectification in both genotypes and reversed close to E_K (WT, −105 ± 5 mV, $n = 4$; TASK-1$^{-/-}$, −107 ± 2 mV, $n = 8$; Fig. 4C). Second, the effect of mAChR activation was recorded under current-clamp conditions. To allow high-frequency burst firing, cells were held at a potential of −72 ± 1 mV ($n = 8$) via DC current injection.

Depolarizing current steps (100–150 pA) evoked a typical burst of two to five action potentials riding on top of a low-threshold calcium spike (Steriade et al., 1997) in both mouse genotypes (Fig. 4, E and F, black traces). The intraburst frequency was 123 ± 2 Hz ($n = 4$) and 126 ± 1 Hz ($n = 4$) for WT and TASK-1$^{-/-}$, respectively. Bath application of muscarine (50 μM) induced a depolarizing shift in membrane potential that was not different between littermates (WT, 23 ± 2 mV, $n = 6$; TASK-1$^{-/-}$, 21 ± 3 mV, $n = 6$). This depolarization was accompanied by a switch in firing mode from burst to tonic generation of action potentials (Fig. 4, E and F, gray traces). The frequency of tonic firing as derived from the first two spikes was 27 ± 4 Hz ($n = 4$) and 32 ± 3 Hz ($n = 4$) for WT and TASK-1$^{-/-}$, respectively. All effects were fully reversible (data not shown). In summary, these data show that despite a reduction of the muscarine-sensitive current component, the functional impact of mAChR activation is not significantly changed in the two mice genotypes.

The Effects of Cannabinoid Ligands on I_{SO} in DLG Neurons and the Specific Involvement of TASK-1. The cannabinoid agonists anandamide (arachidonylethanolamide; 30 μM) and *R*-(+)-WIN 55,212-2 have been suggested as TASK-1-specific blockers, having no effect on TASK-3 channels (Maingret et al., 2001). In contrast, other reports have claimed that on recombinant channels anandamide does not distinguish between TASK-1 and TASK-3 (Berg et al., 2004; Aller et al., 2005). In the present study, anandamide induced a reduction in I_{SO} amplitude at −28 mV by 23 ± 3% ($n = 5$; Fig. 5B, black column) in WT neurons. In TASK-1$^{-/-}$ DLG neurons, the blocking effect of anandamide was abolished, and drug application was accompanied by a 9 ± 6% ($n = 6$; Fig. 5B, gray column) increase in I_{SO} amplitude. The I-V relationship of the anandamide-sensitive current in WT neurons was characterized by outward rectification and reversed at −103 ± 3 mV ($n = 5$; Fig. 5A, black trace). In contrast, the anandamide-sensitive current in TASK-1$^{-/-}$ DLG TC cells was linear and see-sawed around zero ($n = 6$; Fig. 5A, black circles). To confirm these data, we used an anandamide analog (methanandamide; 10 μM) with higher metabolic stability. Whereas application of methanandamide onto WT neurons reduced I_{SO} amplitude by 20 ± 2% ($n = 6$; Fig. 5B, stripped black column), the effect was absent on TASK-1$^{-/-}$ DLG cells (4 ± 6% increase in I_{SO} amplitude; $n = 6$; Fig. 5B, gray stripped column). The I-V relationship of the methanandamide-sensitive current was characterized by outward rectification and a reversal potential at −105 ± 2 mV ($n = 6$; Fig. 5A, gray trace). In TASK-1$^{-/-}$ DLG cells, the methanandamide-sensitive current was linear with near zero amplitude ($n = 6$; Fig. 5A, gray circles). Because anandamide

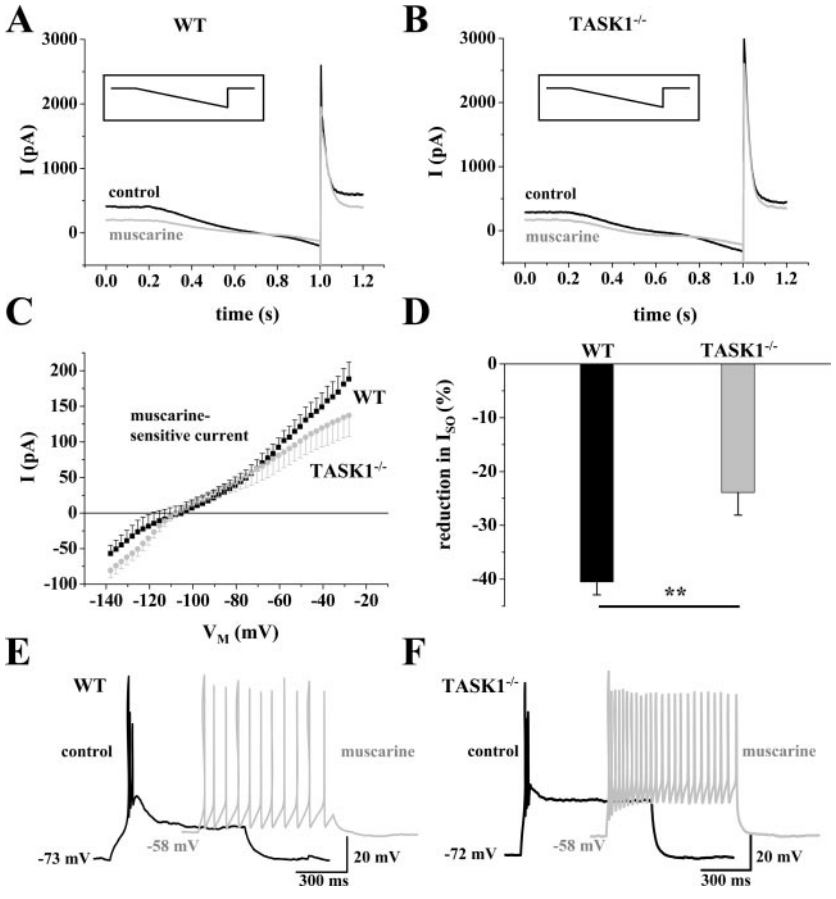

Fig. 4. Muscarine effect on I_{SO} in WT and TASK-1$^{-/-}$ DLG neurons. A and B, membrane responses to ramp protocols (from −28 to −138 mV over 800 ms; see inset) under control conditions (black traces) and during bath application of muscarine (gray traces) in WT (A) and TASK-1$^{-/-}$ DLG cells (B). C, mean I-V relationship of the muscarine-sensitive current was calculated by graphical subtraction of currents during drug action from those under control conditions (i.e., control − muscarine). D, mean bar graph representation of I_{SO} reduction at −28 mV by muscarine in WT (black column) and TASK-1$^{-/-}$ (gray column). E and F, functional consequences of muscarine administration were tested under whole-cell current-clamp conditions in WT (E) and TASK-1$^{-/-}$ (F). DLG TC neurons of both mouse genotypes were held at a potential of 72 ± 1 mV ($n = 8$) by DC current injection. This holding current was not changed during the course of the experiment. Cells were challenged using 100- to 200-pA depolarizing current pulses (800-ms duration). Under control conditions, depolarizing current pulses starting from hyperpolarized membrane potentials evoked typical burst firing (black traces). Addition of muscarine led to a marked depolarization of the membrane potential with a consecutive shift of the activity mode from burst to tonic firing (gray traces).

can be rapidly transformed to arachidonic acid (AA), we next investigated the effect of this eicosanoid on I_{SO} in DLG TC neurons. In both TASK-$1^{-/-}$ and WT DLG cells, AA induced a significant increase in I_{SO} amplitude and was thus very different from the effect of the two anandamide derivatives (WT, 25 ± 6% increase, $n = 5$; TASK-$1^{-/-}$, 32 ± 9%, $n = 7$; data not shown).

Because TASK-3 channels are specifically blocked by divalent cations (Derst et al., 2002; Clarke et al., 2004), we omitted Ca^{2+} and Mg^{2+} from the external recording solution. In both TASK-$1^{-/-}$ and WT DLG cells, I_{SO} amplitudes significantly increased after establishing divalent cation-free conditions (19 ± 2%, $n = 8$ for WT; 18 ± 1%, $n = 4$ for TASK-$1^{-/-}$; Fig. 5D), with the curvature of the I-V relationship of the divalent cation-sensitive current pointing to the contribution of outwardly and inwardly rectifying components. The current reversal was close to E_K (−104 ± 2 mV for WT, Fig. 5C, black trace; −102 ± 3 mV for TASK1$^{-/-}$ mice, Fig. 5C, gray trace). These data demonstrate the absence of TASK-1-specific effects and an unchanged response to a TASK-3-specific experimental maneuver in TASK-$1^{-/-}$ DLG cells.

Electroencephalographic Recordings. To assess possible deficits of TASK-$1^{-/-}$ mice with respect to whole brain function, we recorded ECoG of freely moving TASK-$1^{-/-}$ and WT littermates. TASK-$1^{-/-}$ as well as WT mice expressed very regular field potential patterns on the ECoG without any abnormalities such as polyspike complexes or high-voltage spike activities and showed similar patterns during expression of different behavioral states (e.g., wake and sleep; data not shown). During wake behavioral state, both genotypes revealed predominant frequencies at theta frequency (5–12 Hz). During sleep the ECoG of TASK-$1^{-/-}$ and WT animals was characterized by higher amplitudes compared with the wake state and low-frequency activity at approximately 2 to 4 Hz (data not shown).

Behavioral Observations Indicate a Comparable Sleep-Wake Cycle of TASK-$1^{-/-}$ Mice and Controls. Because the dorsal thalamus plays an important role in the mammalian sleep-wake cycle, we next performed behavioral observations on WT and TASK-$1^{-/-}$ mice. Consistent with the EEG recordings, the behavioral observations offered similar results for both mice genotypes. With respect to sleeping and waking behavior, WT animals were active (addition of moving, rearing, leaning, grooming, and nutrition) and inactive (sleeping and resting) for 44 ± 2 and 56 ± 2% of the day ($n = 5$, repeated measurements; Fig. 6A). The behavior of TASK-$1^{-/-}$ mice was indistinguishable with 43 ± 1% active and 57 ± 1% inactive behavior per 24 h ($n = 5$, repeated measurements; Fig. 6A). Furthermore, the analysis of specific behaviors such as moving, rearing, leaning, grooming, or nutrition showed no statistically significant differences between knockouts and wild-type littermates (Fig. 6B). Likewise, further differentiation of inactive behavior (separation of resting behavior and sleep) displayed no significant differences between the two groups.

Discussion

This study describes novel aspects of TASK-1 channel function in DLG TC neurons and can be summarized as follows: 1) I_{SO} amplitude was reduced and the resting membrane potential was more depolarized in TASK-$1^{-/-}$ cells in comparison with WT; 2) I_{SO} decreased in amplitude with increasing proton concentration. The pK value of current inhibition was shifted to lower pH values in TASK-$1^{-/-}$ neurons compared with WT; 3) The TASK-1 and -3 channel blocker bupivacaine reduced the outwardly rectifying TASK current in TASK-$1^{-/-}$ more effectively than in WT; 4) Muscarine reduced I_{SO} by inhibiting TASK-1 and -3 channels and inwardly rectifying channels. Although this effect was less pronounced in knockouts, neurons switched from burst to

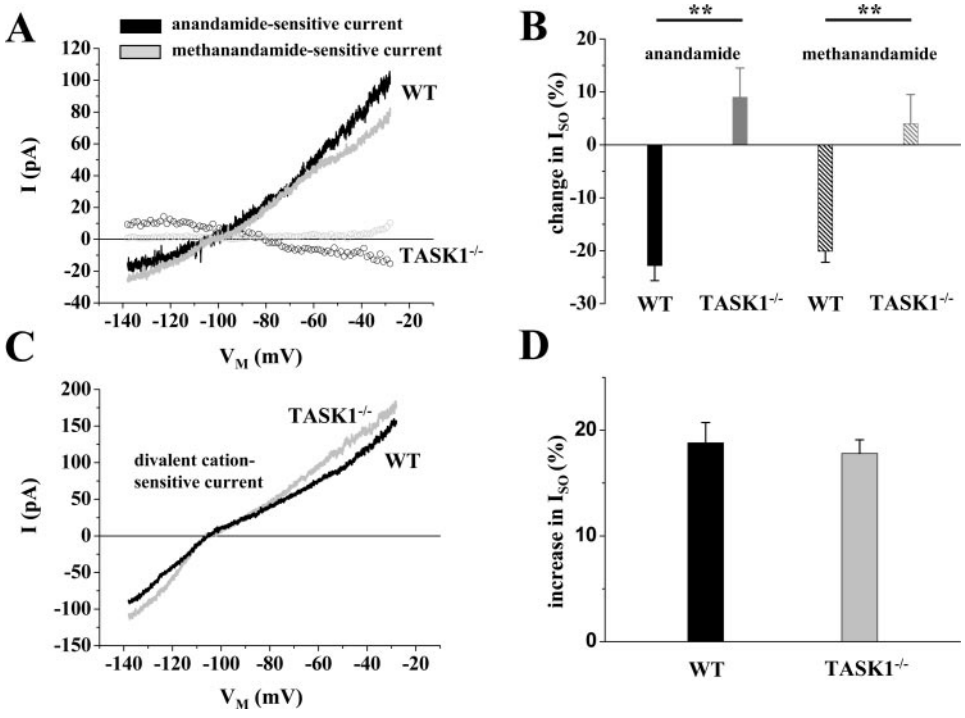

Fig. 5. Specific pharmacological strategies of blocking TASK-1 and TASK-3 channels in DLG TC neurons. A, I-V relationship of anandamide- (black label) and methanandamide-sensitive (gray label) currents in WT (straight lines) and TASK-$1^{-/-}$ (circles). B, mean bar graph representation of I_{SO} changes induced by anandamide (closed columns) and methanandamide (stripped columns) in WT (black label) and TASK-$1^{-/-}$ (gray label). C, I-V relationship of divalent cation-sensitive currents in WT (black line) and TASK-$1^{-/-}$ (gray line). D, mean bar graph representation of I_{SO} induced by removal of divalent cations from the extracellular solution at −28 mV in WT (black column) and TASK-$1^{-/-}$ (gray column).

tonic firing in both TASK-1$^{-/-}$ and WT. 5) Anandamide as well as the more stable methanandamide blocked an outward rectifying TASK current component in WT but was ineffective in TASK-1$^{-/-}$. On the other hand, removal of divalent cations from the extracellular medium, a maneuver to specifically unblock TASK-3 channels, was equally effective in the two genotypes. 6) Consistent with the mild electrophysiological effects of TASK-1 gene knockout in the dorsal thalamus, no noticeable differences between WT and TASK-1$^{-/-}$ mice were found in EEG recordings and in the overall sleep/waking behavior. We conclude 1) that in DLG neurons TASK-1 makes a significant contribution to I_{SO} and 2) that anandamide blocks TASK-1 or TASK-1 and -3 channels in WT cells but not the presumably homomeric TASK-3 channels remaining in the TASK-1$^{-/-}$ DLG TC cells.

TASK Channels in DLG TC Neurons. The TASK channel genes are differentially expressed in the rodent central nervous system (Talley et al., 2001). In rat DLG TC neurons, the current carried by TASK channels is characterized by outward rectification, reversal at E_K, inhibition by extracellular acidification, block by bupivacaine, and down-regulation by activation of mAChR (Meuth et al., 2003). From the data presented here, we estimate that current through TASK-1 homodimers or TASK-1/TASK-3 heterodimers (Czirjak and Enyedi, 2002) contributes approximately one third of the current sensitive to TASK channel modulators in DLG TC neurons. This conclusion is based on the following evidence: 1) Compared with WT, the bupivacaine-sensitive current in TASK-1$^{-/-}$ DLG TC neurons is approximately 35% smaller in amplitude. 2) The difference between bupivacaine-sensitive currents in WT and TASK-1$^{-/-}$ DLG cells at −28 mV is approximately 100 pA. 3) Similar to the effect of bupivacaine, the muscarine-sensitive component is approximately 28% smaller in TASK-1$^{-/-}$ DLG cells. These findings further indicate that bupivacaine (Leonoudakis et al., 1998; Brown, 2000; Buckler et al., 2000) and mechanisms acting downstream of mAChR (Patel and Lazdunski, 2004) influence TASK-1 and TASK-3 channels similarly. Nevertheless, knockout of the TASK-1 gene significantly reduced I_{SO}, resulting in a depolarized resting membrane potential, thereby confirming the persistent activity of native TASK-1 channels and their contribution to the neuronal membrane potential (Duprat et al., 1997). However, in adult cerebellar granule cells, deletion of the TASK-1 protein leaves the magnitude of I_{KSO} unaffected (Aller et al., 2005), whereas deletion of TASK-1 from DLG TC cells produces a decrease in leak conductance. One explanation is that granule cells express more K2P subunit genes at higher levels than DLG TC cells, allowing greater possibilities of compensation (Brickley et al., 2001). Similar considerations may apply to other brain regions because the TASK-1$^{-/-}$ phenotype shows few neurological deficits.

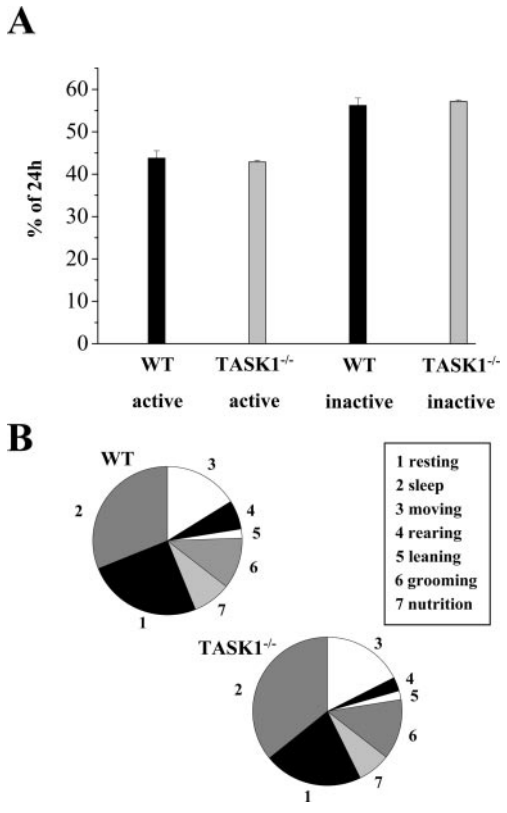

Fig. 6. Behavioral analysis of WT and TASK-1$^{-/-}$. A, mean bar graph representation of active (black columns) and inactive (gray columns) periods in WT and TASK-1$^{-/-}$ (as indicated) in percentage of 24 h. B, pie diagram representation of distinct active (moving, rearing, leaning, grooming, and nutrition) and inactive (resting and sleep) behavior components.

Both TASK1 and TASK3 channels are inhibited by acidification, although over different pH ranges (pK ~7.5 and ~6.7 for TASK-1 and TASK-3, respectively) (Duprat et al., 1997; Kim et al., 2000; Rajan et al., 2000). Tandem-linked heterodimeric TASK channel constructs displayed pH sensitivity (pK ~7.3) closer to that of TASK-1 than TASK-3 (Berg et al., 2004). Consistent with these findings, I_{SO} amplitude in TC cells of WT (TASK-3 + TASK-1; EC_{50} = 6.6) revealed an EC_{50} value that was shifted to a more alkaline pH value in comparison with TASK1$^{-/-}$ (TASK-3 only; EC_{50} = 5.9). Deviation of absolute pK values from those published for heterologously expressed TASK channels and the 90% reduction of I_{SO} at pH 5.0 probably result from the fact that the steady-state current in TC neurons is carried by a number of different ion channels (persistent Na^+ channels, inward rectifier K^+ channels, noninactivating voltage-dependent K^+ channels, TASK channels, and pacemaker channels; S. G. Meuth and T. Budde, unpublished observations) with unknown or undefined pH sensitivity. Changes of the extracellular pH can influence a variety of different conductances and receptors (Kaila and Ransom, 1998), so that additional contributors to the pH effects can be expected.

Endogenous Cannabinoids and Their Actions on TASK Channels of DLG Cells. Human recombinant TASK-1 but not TASK-3 channels are blocked by anandamide (Maingret et al., 2001). However, the situation seems to be more complicated when taking rodent TASK channels into account, because two other groups claim that anandamide blocks both recombinant (rodent) TASK-1 and TASK-3 channels fairly equally at concentrations >1 μM (Berg et al., 2004; Aller et al., 2005). We were surprised to find that TASK-1 channels convey the anandamide-sensitivity of I_{SO} in DLG TC neurons, thereby confirming that the endogenous cannabinoid ligand anandamide compounds selectively block TASK-1 channels (Maingret et al., 2001). This conclusion is confirmed indirectly by the effect of specifically activating TASK-3 channels by removing extracellular divalent cations, which produced indistinguishable effects in the two mouse

genotypes. Anandamide may be rapidly eliminated by enzymatic hydrolysis, leading to the production of AA. The finding that AA induced an increase in I_{SO} rather than a reduction further confirms the specific action of anandamide. Although we have no intuitive explanation for this selectivity of anandamide for TASK-1 in native membranes, the following findings should be taken into account: 1) At higher concentrations (10 μM), recombinant rodent TASK-1 channels are more sensitive to anandamide than rodent TASK-3 channels (Berg et al., 2004). 2) The anandamide-sensitive current components in rat and mouse DLG TC neurons are similar: they outwardly rectify, reverse at E_K, and constitute 22 ± 2% (n = 4) and 23 ± 3% (n = 5) of I_{SO}, respectively. These findings may point to subtle cell type-specific influences. 3) TASK channels are regulated by adapter proteins and phosphatidylinositol-4,5-bisphosphate (Czirjak et al., 2001; Rajan et al., 2002; Chemin et al., 2003; Lopes et al., 2005), thereby indicating complex interplay between multiple factors. 4) TASK-1$^{-/-}$ mice have changed responses to the cannabinoid ligand WIN55212-2 (Linden et al., 2004); the analgesic, sedative, and hypothermic effects of WIN55212-2 are reduced in TASK-1$^{-/-}$ mice, implicating channels containing TASK-1 in supraspinal pain pathways, for example, in the thalamus. This behavioral result confirms that endogenous cannabinoid ligands certainly have the potential to influence cell excitability by acting close to TASK-1 and/or TASK-3 channels in vivo.

TASK-1 Function in the Thalamocortical System. The resting membrane potential of thalamic relay neurons is in the range of −70 mV and has been attributed to currents through leak channels ($I_{K\text{-leak}}$ and $I_{Na\text{-leak}}$), pacemaker channels (I_h), inwardly rectifying K^+ currents (I_{KIR}), and voltage-dependent channels active below threshold (I_A and I_T) (Williams et al., 1997; Zhan et al., 1999). TASK-1 contributes ~3 mV hyperpolarization to V_{rest} and partially counterbalances the depolarizing influence of I_h. Strong extracellular acidification completely inhibited current through TASK-1 and -3 channels and resulted in a marked depolarization of V_{rest}, indicating some tens of mV hyperpolarizing influence of TASK channels. The value of the prevailing membrane potential in TC neurons is outstandingly important for thalamic function because these cells display burst activity and tonic firing at hyperpolarized and depolarized values of the membrane potential, respectively (Steriade et al., 1997). The burst mode of activity is characterized by two to six action potentials on the ridge of a low threshold calcium spike and occurs during natural sleep and absence epilepsy. Generation of single action potentials can be observed during wakefulness (Steriade et al., 1997). The shift between the two activity modes is mediated by transmitters of the ascending brain stem system (e.g., ACh) acting on $I_{K\text{-leak}}$ (McCormick, 1992). TASK-1 and TASK-3 channels have been shown to constitute the mAChR-sensitive leak current in TC neurons (Meuth et al., 2003). However, removal of TASK-1 is not sufficient to disrupt the mAChR-dependent switch from burst to tonic firing in DLG TC neurons in situ. Although the tonic firing frequency of TASK-1$^{-/-}$ TC neurons tends toward higher frequencies during ACh application (27 and 32 Hz for WT and TASK-1$^{-/-}$, respectively), a comparison with cells from standard C57/BL6 wild-type mice revealed no significant differences (32 ± 2 Hz, n = 7, under identical recording conditions), thereby indicating similar tonic firing properties in different mouse genotypes. In accordance with this finding, no behavioral deficits related to the function of the thalamocortical system (e.g., overall EEG pattern and sleeping/waking behavior) could be observed for TASK-1$^{-/-}$ mice. However, the idea that sleep deprivation or some other induced stress would reveal functional differences between WT and TASK-1$^{-/-}$ cannot be excluded. We anticipate that TASK-3 and TASK-1/TASK-3 double or perhaps TASK-1/TASK-3/TWIK-1 triple knockouts will be needed to assess the full impact of K2P channel activity on thalamic function.

Acknowledgments

We thank I. Preugschat-Gumprecht (Heidelberg), R. Ziegler (Magdeburg) and A. Jahn (Magdeburg) for excellent technical assistance. W.W. thanks Prof. Dr. H. Monyer for generous support.

References

Aller MI, Veale EL, Linden AM, Sandu C, Schwaninger M, Evans LJ, Korpi ER, Mathie A, Wisden W, and Brickley SG (2005) Modifying the subunit composition of TASK channels alters the modulation of a leak conductance in cerebellar neurons. *J Neurosci* **25:**11455–11467.

Bayliss DA, Sirois JE, and Talley EM (2003) The TASK family: two-pore domain background K^+ channels. *Mol Intervent* **3:**205–219.

Berg AP, Talley EM, Manger JP, and Bayliss DA (2004) Motoneurons express heteromeric TWIK-related acid-sensitive K^+ (TASK) channels containing TASK-1 (KCNK3) and TASK-3 (KCNK9) subunits. *J Neurosci* **24:**6693–6702.

BoSmith RE, Briggs I, and Sturgess NC (1993) Inhibitory actions of ZENECA ZD7288 on whole-cell hyperpolarization activated inward current (If) in guinea-pig dissociated sinoatrial node cells. *Br J Pharmacol* **110:**343–349.

Brickley SG, Revilla V, Cull-Candy SG, Wisden W, and Farrant M (2001) Adaptive regulation of neuronal excitability by a voltage-independent potassium conductance. *Nature (Lond)* **409:**88–92.

Brown DA (2000) Neurobiology: the acid test for resting potassium channels. *Curr Biol* **10:**R456–R459.

Buckler KJ, Williams BA, and Honore E (2000) An oxygen-, acid- and anaesthetic-sensitive TASK-like background potassium channel in rat arterial chemoreceptor cells. *J Physiol (Lond)* **525:**135–142.

Chemin J, Girard C, Duprat F, Lesage F, Romey G, and Lazdunski M (2003) Mechanisms underlying excitatory effects of group I metabotropic glutamate receptors via inhibition of 2P domain K^+ channels. *EMBO (Eur Mol Biol Organ) J* **22:**5403–5411.

Clarke CE, Veale EL, Green PJ, Meadows HJ, and Mathie A (2004) Selective block of the human 2-P domain potassium channel, TASK-3 and the native leak potassium current, IKSO, by zinc. *J Physiol (Lond)* **560:**51–62.

Czirjak G and Enyedi P (2002) Formation of functional heterodimers between the TASK-1 and TASK-3 two-pore domain potassium channel subunits. *J Biol Chem* **277:**5426–5432.

Czirjak G and Enyedi P (2003) Ruthenium red inhibits TASK-3 potassium channel by interconnecting glutamate 70 of the two subunits. *Mol Pharmacol* **63:**646–652.

Czirjak G, Petheo GL, Spat A, and Enyedi P (2001) Inhibition of TASK-1 potassium channel by phospholipase C. *Am J Physiol* **281:**C700–C708.

Derst C, Liu GX, Musset B, Rajan S, Preisig-Müller R, and Daut J (2002) Molecular analysis of divalent cation sensitivity of TASK channels. *Pflueg Arch Eur J Physiol* **443 (Suppl 2):**P44–P10.

Dixon WJ and Massey FJ (1969) *Introduction to Statistical Analysis*, McGraw-Hill Companies, New York.

Duprat F, Lesage F, Fink M, Reyes R, Heurteaux C, and Lazdunski M (1997) TASK, a human background K^+ channel to sense external pH variations near physiological pH. *EMBO (Eur Mol Biol Organ) J* **16:**5464–5471.

Kaila K and Ransom BR (1998) *pH and Brain Function*, Wiley-Liss, New York.

Kang D, Han J, Talley EM, Bayliss DA, and Kim D (2004) Functional expression of TASK-1/TASK-3 heteromers in cerebellar granule cells. *J Physiol (Lond)* **554:**64–77.

Kim Y, Bang H, and Kim D (2000) TASK-3, a new member of the tandem pore K^+ channel family. *J Biol Chem* **275:**9340–9347.

Kindler CH, Yost CS, and Gray AT (1999) Local anesthetic inhibition of baseline potassium channels with two pore domains in tandem. *Anesthesiology* **90:**1092–1102.

Leonoudakis D, Gray AT, Winegar BD, Kindler CH, Harada M, Taylor DM, Chavez RA, Forsayeth JR, and Yost CS (1998) An open rectifier potassium channel with two pore domains in tandem cloned from rat cerebellum. *J Neurosci* **18:**868–877.

Lesage F and Lazdunski M (2000) Molecular and functional properties of two-pore-domain-potassium channels. *Am J Physiol* **279:**F793–F801.

Linden AM, Aller MI, Vekovischeva O, Leppa E, Rosenberg PH, Wisden W, and Korpi ER (2004) Sensitivity of K^+ channel task-1 deficient mice to anesthetics isoflurane and propofol. *Soc Neurosci Abstr* (http://sfn.scholarone.com/itin2004/main.html?new_page_id=126&abstract_id=1918&p_num=966.1&is_tech=0).

Lopes CM, Rohacs T, Czirjak G, Balla T, Enyedi P, and Logothetis DE (2005) PIP2 hydrolysis underlies agonist-induced inhibition and regulates voltage gating of two-pore domain K^+ channels. *J Physiol (Lond)* **564:**117–129.

Maingret F, Patel AJ, Lazdunski M, and Honore E (2001) The endocannabinoid anandamide is a direct and selective blocker of the background K^+ channel TASK-1. *EMBO (Eur Mol Biol Organ) J* **20:**47–54.

McCormick DA (1992) Neurotransmitter actions in the thalamus and cerebral cortex and their role in neuromodulation of thalamocortical activity. *Prog Neurobiol* **39:**337–388.

Meadows HJ and Randall AD (2001) Functional characterisation of human TASK-3, an acid-sensitive two-pore domain potassium channel. *Neuropharmacology* **40:** 551–559.

Meuth SG, Budde T, Kanyshkova T, Broicher T, Munsch T, and Pape H-C (2003) Contribution of TWIK-related acid-sensitive K^+ channel 1 (TASK1) and TASK3 channels to the control of activity modes in thalamocortical neurons. *J Neurosci* **23:**6460–6469.

Millar JA, Barratt L, Southan AP, Page KM, Fyffe RE, Robertson B, and Mathie A (2000) A functional role for the two-pore domain potassium channel TASK-1 in cerebellar granule neurons. *Proc Natl Acad Sci USA* **97:**3614–3618.

Patel AJ and Honore E (2001) Properties and modulation of mammalian 2P domain K^+ channels. *Trends Neurosci* **24:**339–346.

Patel AJ and Lazdunski M (2004) The 2P-domain K^+ channels: role in apoptosis and tumorigenesis. *Pflueg Arch Eur J Physiol* **448:**261–273.

Plant LD, Rajan S, and Goldstein SA (2005) K2P channels and their protein partners. *Curr Opin Neurobiol* **15:**326–333.

Rajan S, Plant LD, Rabin ML, Butler MH, and Goldstein SA (2005) Sumoylation silences the plasma membrane leak K^+ channel K2P1. *Cell* **121:**37–47.

Rajan S, Preisig-Muller R, Wischmeyer E, Nehring R, Hanley PJ, Renigunta V, Musset B, Schlichthorl G, Derst C, Karschin A, et al. (2002) Interaction with 14-3-3 proteins promotes functional expression of the potassium channels TASK-1 and TASK-3. *J Physiol (Lond)* **545:**13–26.

Rajan S, Wischmeyer E, Xin Liu G, Preisig-Muller R, Daut J, Karschin A, and Derst C (2000) TASK-3, a novel tandem pore domain acid-sensitive K^+ channel. An extracellular histidine as pH sensor. *J Biol Chem* **275:**16650–16657.

Steriade M, Jones EG, and McCormick DA (1997) *Thalamus*, Elsevier, Amsterdam.

Talley EM, Lei Q, Sirois JE, and Bayliss DA (2000) TASK-1, a two-pore domain K^+ channel, is modulated by multiple neurotransmitters in motoneurons. *Neuron* **25:**399–410.

Talley EM, Solorzano G, Lei Q, Kim D, and Bayliss DA (2001) CNS distribution of members of the two-pore-domain (KCNK) potassium channel family. *J Neurosci* **21:**7491–7505.

Williams SR, Toth TI, Turner JP, Hughes SW, and Crunelli V (1997) The 'window' component of the low threshold Ca^{2+} current produces input signal amplification and bistability in cat and rat thalamocortical neurones. *J Physiol (Lond)* **505:**689–705.

Zhan XJ, Cox CL, Rinzel J, and Sherman SM (1999) Current clamp and modeling studies of low-threshold calcium spikes in cells of the cat's lateral geniculate nucleus. *J Neurophysiol* **81:**2360–2373.

Address correspondence to: Dr. Thomas Budde, Institut für Experimentelle Epilepsieforschung, Westfälische Wilhelms-Universität Münster, Hüfferstr. 68, D-48149 Münster, Germany. E-mail: tbudde@uni-muenster.de